Received: 18 November 2020 | Revised: 3 March 2021 | Accepted: 1 May 2021

DOI: 10.1111/nan.12730

Neuropathology and Applied Neurobiology WILEY

ORIGINAL ARTICLE

Inflammation, fibrosis and skeletal muscle regeneration in LGMDR9 are orchestrated by macrophages

Heike Kölbel[1] | Corinna Preuße[2,3] | Lukas Brand[1] | Arpad von Moers[4] | Adela Della Marina[1] | Markus Schuelke[5] | Andreas Roos[1] | Hans-Hilmar Goebel[2,6] | Ulrike Schara-Schmidt[1] | Werner Stenzel[2]

[1]Department of Neuropaediatrics, Neuromuscular Centre, Universitätsmedizin Essen, Germany

[2]Department of Neuropathology, Charité - Universitätsmedizin, corporate member of Freie Universität Berlin and Humboldt-Universität zu Berlin, Berlin, Germany

[3]Department of Neurology with Institute for Translational Neurology, University Hospital Münster, Münster, Germany

[4]Department of Paediatrics and Neuropaediatrics, DRK Klinikum Westend, Berlin, Germany

[5]Department of Neuropediatrics, Charité - Universitätsmedizin Berlin, corporate member of Freie Universität Berlin and Humboldt-Universität zu Berlin, Berlin, Germany

[6]Department of Neuropathology, Universitätsmedizin Mainz, Germany

Correspondence
Werner Stenzel, Department of Neuropathology, Charité – Universitätsmedizin Berlin, corporate member of Freie Universität Berlin and Humboldt-Universität zu Berlin, Charitéplatz 1, 10117 Berlin, Germany.
Email: werner.stenzel@charite.de

Funding information
European Regional Development Fund (ERDF)

Abstract

Aims: Variable degrees of inflammation, necrosis, regeneration and fibrofatty replacement are part of the pathological spectrum of the dystrophic process in alpha dystroglycanopathy LGMDR9 (FKRP-related, OMIM #607155), one of the most prevailing types of LGMDs worldwide. Inflammatory processes and their complex interplay with vascular, myogenic and mesenchymal cells may have a major impact on disease development. The purpose of our study is to describe the specific immune morphological features in muscle tissue of patients with LGMDR9 to enable a better understanding of the phenotype of muscle damage leading to disease progression.

Methods: We have analysed skeletal muscle biopsies of 17 patients genetically confirmed as having LGMDR9 by histopathological and molecular techniques.

Results: We identified CD206$^+$ MHC class II$^+$ and STAT6$^+$ immune-repressed macrophages dominating the endomysial infiltrate in areas of myofibre regeneration and fibrosis. Additionally, PDGFRβ^+ pericytes were located around MHC class II$^+$ activated capillaries residing in close proximity to areas of fibrosis and regenerating fibres. Expression of VEGF was found on many regenerating neonatal myosin$^+$ fibres, myofibres and CD206$^+$ macrophages also co-expressed VEGF.

Conclusion: Our results show characteristic immune inflammatory features in LGMDR9 and more specifically shed light on the predominant role of macrophages and their function in vascular organisation, fibrosis and myogenesis. Understanding disease-specific immune phenomena potentially inform about possibilities for anti-fibrotic and anti-inflammatory therapeutic strategies, which may complement Ribitol replacement and gene therapies for LGMDR9 that may be available in the future.

KEYWORDS
alpha dystroglycan, CD206, fibrosis, inflammation, LGMDR9, macrophages, regeneration, VEGF

Ulrike Schara-Schmidt and Werner Stenzel shared last authorships.

INTRODUCTION

Alpha-dystroglycanopathy (LGMDR9 formally LGMD2I) is one of the most prevalent limb girdle muscular dystrophies worldwide, specifically in certain countries such as northern England and Denmark,[1,2] with currently more than 150 mutations described.[3] The spectrum of LGMDR9 phenotypes ranges from infants with an early presentation and a Duchenne-like disease course including cardiomyopathy and respiratory failure, to milder phenotypes characterised by later onset of the disease and a relatively slow progression.[4] LGMDR9 is caused by mutations in the *FKRP* gene encoding the so-called fukutin-related protein, a ribitol-5-phosphate (RboP) transferase involved in cellular cytidine 5′-diphosphate (CDP)-ribitol synthesis, a process crucial for the extension of the glycan chain of α-dystroglycan (α-DG).[5] The aetiopathogenesis of the disease involves a defective O-glycosylation of α-DG, an integral transmembrane protein of the sarcolemma.[6] Mature α-DG consists of a C-terminal domain and a mucin-domain that is modified by FKRP and other glycosyltransferases via O-glycosylation for a regular function of oligosaccharides and the extracellular matrix (EMC), inevitably causing muscle fibre instability during mechanically demanding conditions.[3,7,8]

In muscular dystrophies, inflammatory features were previously described, and their specific role was shown to promote muscle injury and/or repair in Duchenne muscular dystrophy (DMD).[9,10] Studies aimed at characterising the immune cells that invade dystrophic muscle revealed that $CD4^+$ and $CD8^+$ T cells, macrophages, eosinophils and natural killer T cells infiltrate both human and mouse dystrophic skeletal muscle.[9] It is likely that a part of the muscle injury, which occurs in α-DG-deficiency results from a secondary damage caused by an immune response to dystrophic muscle, rather than mechanical damage to the weakened muscle *per se*. However, the inflammatory characteristics in LGMDR9 have scantily been described.[11] Importantly, therapeutic interventions positively modulating the balance between diverse macrophage populations, like corticosteroids in DMD patients, may potentially rescue the injury of devastating immune mechanisms in LGMDR9.

In light of the upcoming new treatment options for LGMDR9 patients with gene therapy or Ribitol replacement,[12,13] a precise determination of underlying pathophysiological processes is crucial. To systematically address this gap of knowledge, we combined analysis of clinical information with immunological findings in LGMDR9 patient-derived skeletal muscle biopsies focussing on immune-inflammatory characteristics detectable in the skeletal muscle tissues.

PATIENTS, MATERIALS AND METHODS

Patients

Among a cohort of 237 LGMD patients, 21 patients with genetically confirmed LGMDR9 (FKRP-related) were recruited by the Department of Neuropaediatrics, Neuromuscular Centre, University Hospital Essen. For 16/21 patients, skeletal muscle biopsies were available. For one of those we did not obtain consent from the parents, one further patient could be included from the Department of Neuropathology, Charité—Universitätsmedizin and one patient by the DRK Klinikum Westend, Berlin, respectively. Thus, in total, 17 patients (11 females and 6 males) were included. Clinical features of these patients and all available paraclinical as well as molecular genetic data are summarised in Table 1. Molecular genetic findings from patients 1 to 4 have been published before.[14]

Morphological analyses were performed at the Department of Neuropathology, Charité-Universitätsmedizin, Berlin.

Three control biopsies (non-disease control [NDC] patients' biopsies; age range between 2 and 14 years) with non-specific muscular complaints were included. They presented with unremarkable clinical findings, normal serum CK, absence of any systemic inflammation and absence of morphological abnormalities in their skeletal muscle biopsies. Biopsies had been performed to ultimately exclude any morphological abnormality, and this had been done by means of extensive examination including enzyme histochemistry, immunohistochemistry and electron microscopy.

All biopsies were obtained for diagnostic procedures and prior to any treatment. All specimens had been cryopreserved at −80°C.

Histology, enzyme histochemistry and immunohistochemistry

Cryostat sections of 7 μm thick were stained by routine stains and enzyme histochemical preparations including modified Gömöri trichrome, ATP-ases at pH 4.3, 4.6 and 9.4, acid phosphatase, non-specific esterase, PAS, Oil-red-O, NADH-TR, COX-SDH and SDH. Immunohistochemistry was done with antibodies against CD4 (Zytomed, clone SP35, ready-to-use), CD8 (DAKO, clone C8/144B, 1:100), CD56 (Serotec/MCA591, clone ERIC-1, 1:400), CD68 (DAKO, clone EBM11, 1:100), CD45 (DAKO, clone 2B11, 1:400), CD206 (Acris, clone 7–450, 1:500), CollagenVI (Chemicon, clone VI-26, 1:200), DAP12 (TYROBP; Novus Biologicals NBP1-85313, 1:100), alpha-dystroglycan (Millipore #05-593, clone IIH6C4, 1:10), MHC class I (DAKO, clone W6/32 1:1000), MHC class II (DAKO, clone CR3/43, 1:100), nMyHc (Novocastra, clone NB-MHCn, 1:20), developmental MyHC (Novocastra, clone NB-MHCd, 1:50), STAT6 (R&D, clone 253906, 1:50), VEGF (Abcam, clone 2Ar2, 1:30), C5b-9 (DAKO/M777, clone aE11, 1:100), nNOS (Biomol, rabbit polyclonal, 1:100), PDGFRβ (Santa Cruz SC338 C-20, rabbit polyclonal, 1:30) and Siglec-1 (Millipore, clone 5F1.1; 1:50).

Stains were performed using the iVIEW-Ventana DAB (diaminobenzidine)-Detection Kit (Ventana, Tucson, Arizona, 85755 USA). Appropriate biotinylated secondary antibodies were used, and visualisation of the reaction product was carried out on a Benchmark XT immunostainer (Ventana) in a standardised manner. In addition, we used normal muscle tissues as negative control (or physiological internal control e.g. staining of MHC class I positivity of capillaries) for all reactions.

TABLE 1 Summary of all relevant clinical data

Patient# sex	Mutations on both alleles [NM_024301.5] [NP_077277.1]	Motor function [last visit]	First symptoms	Motor development	Age at onset	Interval until biopsy	Age at biopsy	CK [U/l] level at biopsy	Orthopaedic symptoms	Cardiac symptoms	Respiratory symptoms
1 female	c.826C>A | c.826C>A p.(Leu276Ile) | p.(Leu276Ile)	walking	tip-toe walking	regular	2 y	8 y	10 y	7795	contractures, hyperlordosis	none	none
2 female	c.826C>A | c.826C>A p.(Leu276Ile) | p.(Leu276Ile)	walking	reduced head control	regular	9 m	1.5 y	2.3 y	4870	contractures, hyperlordosis	none	restrictive ventilatory disorder
3 female	c.826C>A | c.390_391insTACC p.(Leu276Ile) | p.(Asp131 Tyrfs*7)	wheelchair dependent	reduced spontaneous movements	delayed	1 m	8 y	8.1 y	849	contractures, hyperlordosis	dilatative cardiomyopathy	none
4 female	c.826C>A | c.826C>A p.(Leu276Ile) | p.(Leu276Ile)	walking	delayed motor development	regular	10 m	1.5 y	2.4 y	n/a	none	none	none
5 male	c.1087G>T | c.1087G>T p.(Val363Leu) | p.(Val363Leu)	wheel chair dependent	elevated CK	regular	7 y	4.5y	11.5 y	3665	contractures, hyperlordosis	dilatative cardiomyopathy	restrictive ventilatory disorder
6 female	c.826C>A | c.826C>A p.(Leu276Ile) | p.(Leu276Ile)	walking	muscle cramps	regular	6 y	3 y	9 y	21000	contractures, hyperlordosis	none	none
7 male	c.826C>A | c. 947C>G p.(Val363Leu) | p.(Pro316Arg)	walking	muscle pain	regular	5 y	1 y	6 y	2156	contractures, scoliosis	dilative cardiomyopathy	none
8 female	c.826C>A | c.826C>A p.(Leu276Ile) | p.(Leu276Ile)	walking	muscle pain	regular	13 y	2.5 y	15.5 y	7828	scoliosis	none	none
9 female	c.826C>A | c.826C>A p.(Leu276Ile) | p.(Leu276Ile)	walking	muscle pain	regular	7 y	2 y	9 y	12981	contractures, hyperlordosis	dilative cardiomyopathy	none
10 female	c.826C>A | c.826C>A p.(Leu276Ile) | p.(Leu276Ile)	walking	muscular hypotonia	regular	2 m	3 y	3.2 y	7038	contractures, scoliosis	none	restrictive ventilatory disorder
11 male	c.826C>A | c.826C>A p.(Leu276Ile) | p.(Leu276Ile)	walking	elevated CK	delayed	5 y	2 y	7 y	2420	contractures, hyperlordosis	none	restrictive ventilatory disorder
12 male	c.826C>A | c.214C>T p.(Leu276Ile) | p.(Gln72*)	walking	tip-toe walking	regular	4 y	2 y	6 y	7149	none	none	none
13 female	c.826C>A (maternal) | c.341C>G & c.1384C>T (paternal) p.(Leu276Ile) | p.(Ala114Gly) & p.(Pro462Ser)	walking	elevated CK	regular	7 m	0.5 y	1.1 y	4577	contractures, hyperlordosis	none	restrictive ventilatory disorder
14 female	c.826C>A | c.1000G>T c.826C>A | p.(Glu334*)	walking	muscle weakness	regular	2 y	4,5 y	6.6 y	6224	contractures, hyperlordosis	none	none
15 male	c.826C>A | c.826C>A p.(Leu276Ile) | p.(Leu276Ile)	walker	exercise intolerance	delayed	4 y	3 y	7 y	8418	contractures, rigid spine	none	none
16 female	c.826C>A | c.826C>A p.(Leu276Ile) | p.(Leu276Ile)	walking	exercise intolerance	regular	6 y	11 y	17 y	11201	none	none	none
17 male	c.826C>A | c.1170_1171del p.(Leu276Ile) | p.(Gly391Leufs*72)	wheelchair dependent	head drop	regular	21 m	0 m	21 m	8849	contractures, mild scoliosis, rigid spine	none	none

Abbreviations: CK, creatine kinase; m: months; y: years.

Immunostaining for fluorescent markers was performed in staining chambers after fixation in acetone for 10 min. The sections were then blocked with the appropriate serum (1:10 in PBS) dependent on the source of the secondary antibody, and incubated with the aforementioned primary antibodies over night at 4°C or for 1 h at RT. After a washing step, the secondary antibody was added for 1 h. For double immune staining of CD206&MHCneo, CD206&STAT6, PDGFRβ&MHC-II, nMyHc&VEGF, DAP12&CD206, with the purpose to show co-localisation of two cellular structures was used. The above-mentioned protocol was performed using the first primary antibody and afterwards the same protocol was repeated with the second primary antibody and appropriate secondary antibodies. Double staining of $CD206^+$ macrophages (visualised with DAB; brown reaction product) and regenerating muscle fibres close-by was visualised by AEC (red reaction) of nMyHc. After a final washing step, the sections were aqueously mounted and stored at 4°C.

Semi-quantitative scoring of muscle pathology features adapted from Wedderburn et al[15]

For quantification of $CD4^+$ or $CD8^+$ T cells, $CD68^+$ as well as $CD206^+$ macrophages, $CD20^+$ B cells, $CD138^+$ plasma cells and C5b-9 on capillaries or sarcolemmal surfaces, we performed a cell-specific count of randomly selected 10 high-power fields (HPF). For the evaluation of sarcolemmal MHC cl. I and MHC cl. II staining results, we performed a quantification per 100 muscle fibres (Table S1).

Regeneration was scored as 1 = single diffusely distributed regenerating neonatal myosin + myocytes, 2 = focally accumulating clusters of regenerating neonatal myosin + myocytes and 3 = multifocal clusters of neonatal myosin + myocytes.

In addition, we added a quantification based on evaluation of laminin 5 and neonatal myosin heavy chain positive fibres/100 fibres (Table S1).

Fibrosis was scored as 1 = enlarged perimysium only, 2 = additional endomysial mild fibrosis, 3 = additional multifocal endomysial fibrosis, 4 additional strong endomysial fibrosis, based on EvG and Gömöri trichrome stains.

Necrotic fibres were counted in Gömöri trichrome and non-specific esterase-stained slides per 100 fibres (Table S1).

Quantitative real-time polymerase chain reaction (qPCR)

RNA was extracted from whole muscle tissue using the trizol/chloroform method, according to the manufacturer's instruction (Invitrogen). Thereafter, RNA was re-suspended and the concentration of total RNA was photometrically determined with a TECAN fluorescence plate reader (Tecan). The RNA was reverse-transcribed using the High-Capacity cDNA Archive Kit (Applied Biosystems), according to the manufacturer's protocol, using 2 µg of total RNA per sample as previously described.[16] For qPCR reactions, 20 ng of cDNA was used. All experiments were run as triplicates and each run contained the reference gene (*PGK1*) as internal control. The expression (mean Ct value) of this reference gene was comparable in all analysed samples, including non-diseased controls, and unaffected by duration of the disease. To exclude loading differences and variations between different runs, all target genes were normalised to expression of *PGK1*. For analysis, the Applied Biosystems™ QuantStudio™ 6 Flex Real-Time PCR System (ThermoFischer, Waltham, MA; USA) was used. Running conditions were as follows: 95°C 0:20, 95°C 0:01, 60°C 0:20; 45 cycles (values above 40 cycles were defined as not expressed). The qPCR assay identification numbers are as follows:

CCL18 (HS00268113_m1), *CD4* (Hs01058407_m1), *CD8A* (Hs00233520_m1), *MRC1* (CD206, Hs00267207_m1), *CLEC10A* (CD301, HS00197107_m1), *COX2* (Hs00153133_m1), *IFNG* (Hs00989291_m1), *IL1B* (Hs01555410_m1), *IL6* (Hs00985639_m1), *IL12B* (Hs01011518_m1),*IL13* (Hs99999038_m1), *IL17A* (Hs00174383_m1), *IL21* (Hs00222327_m1), *INOS* (Hs01075529_m1), *PGK* (Hs99999906_m1), *POSTN* (Hs01566750_m1), *P4HA1* (Prolin-L, Hs00990001_m1), *STAT1* (Hs01013989_m1), *STAT3* (Hs00374280_m1), *STAT6* (Hs00598625_m1), *TGFB1* (Hs00998133_m1) and *TNFA* (Hs00174128_m1).

Data are represented as fold change to show gene expression of the respective markers of LGMDR9 patients compared to non-diseased control patients' biopsies or as ΔCT for not expressed markers (*IL12*, *IL13*, *IL17*, *IL21* and *IFNG*). All values are presented as scattered dot plots with Box–Whiskers plot overlay with means and standard deviation. Gene expression analysis was done using a pre-determined set of genes of interest related to fibrosis and inflammation.[16]

Statistics

The Mann–Whitney U test was applied to analyse quantitative differences of mRNA transcripts. The Kruskal–Wallis one-way ANOVA test was applied to analyse cell counts, using Bonferroni correction of the post hoc tests. The level of significance was set at $p < 0.05$. Statistics were calculated with the GraphPad Prism 8.4.3 software (GraphPad Software, Inc.).

RESULTS

Clinical data of patients

We included 17 genetically confirmed LGMDR9 patients and studied their skeletal muscle biopsy samples. Patients mostly presented with ankle contractures (12/17) and spinal deformity, like scoliosis/rigid spine and lumbar hyperlordosis (13/17). 3/17 patients lost the ability of free walking during the disease course (12, 16, 21 years of age); 4/17 patients were treated with ACE inhibitors and/or beta blockers (13, 14, 17, 17 years of age). 5/17 patients developed a

restrictive ventilatory disorder, at the earliest 3 years after onset of the disease (10, 13, 15, 17, 21 years of age). CK levels were increased in all patients. None of our patients received steroids or immune modulatory therapies prior to muscle biopsy, age at muscle biopsy was 14 months–18 years. An overview of all clinical characteristics is given in Table 1.

Morphological characteristics of patients with LGMD are characterised by focal inflammation and endomysial fibrosis

To assess the involvement of skeletal muscle in disease, we analysed general morphological alterations in all 17 biopsies. Small, mostly rounded fibres and an increased fibre size variation with prominent fibrosis in the endomysium as well as enlargement of the perimysium and foci of regeneration with small basophilic (on H&E; not shown) fibres with large nuclei were identified in all biopsies. Clusters of regenerating fibres were admixed with many macrophages and some lymphocytes (Figure 1). Sarcolemmal utrophin staining was present on muscle fibres in all patients with a focal character in areas of regeneration. Additional morphological changes comprised a widening of the perimysium and endomysium with prominent fibrosis, as shown by Gömöri trichrome (Figure 1A) and EvG stains (Figure 1B). We performed a semi-quantitative evaluation of inflammation, fibrosis and regeneration which is shown in Table 2 and Table S1. Most specimens had moderate numbers and small foci of regenerating muscle fibres based on myosin heavy chain neonatal and developmental positivity. Fibrosis based on EvG and Gömöri trichrome stains of endo- and perimysial areas was mild or moderate with focal character associating with foci of regeneration in most specimen as well (Table 2, Table S1).

Additionally, we demonstrated that the staining of αDG protein was altered in all patients, either showing complete absence (Figure 1C) or a mosaic pattern of αDG-positive and αDG-negative fibres in contrast to a non-disease control (NDC) patients' biopsy (Figure 1C inlay). A correlation between αDG protein alterations and clinical severity, and extent of inflammatory/dystrophic changes in the biopsies could not be found. The above-mentioned regenerating foci were visualised by CD56 (Figure 1E), nMyHc (Figure 1F) and MHC developmental (not shown), and immaturity of the fibres is also demonstrated by the absence of nNOS from the sarcolemma (Figure 1D). There was no complement deposition on any of the sarcolemmal structures and none on capillaries in any biopsies (C5b-9 staining, not shown, counting see Table S1).

Infiltrates are characterised by alternative activated macrophages

Infiltrates consisted of lymphocytes including $CD4^+$ T cells predominantly in the regenerating foci (Figure 2A) while clusters of $CD8^+$ T cells (Figure 2B) were found among the regenerating fibres but not elsewhere. The vast majority of $CD68^+$ macrophages (Figure 2C)

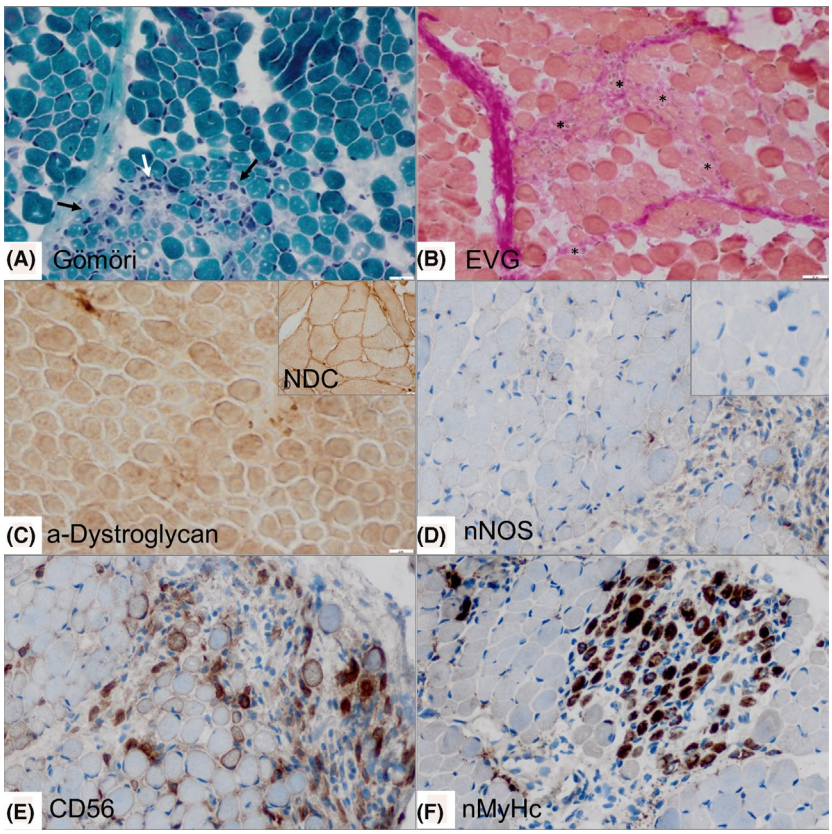

FIGURE 1 General histological features in patients with LGMDR9. Foci of regeneration (black arrow) were admixed with immune cells (white arrow) and endomysium with increased fibrosis (*) in Gömöri (A) and EvG (B) staining. Staining of DG protein fragments was altered (C) when compared to NDC (C, inlay). Staining of nNOS demonstrated absence on the fibres (D) and regenerating foci were visualised by CD56 (E) and MHC neonatal (F). Original magnification 200×

TABLE 2 Summary semi-quantitative score of all morphological hallmarks of the cohort examined herein

	Score	N=17
Inflammation	0 = absent	0% (0)
	1 = focal low	41% (7)
	2 = focal moderate, multifocal sporadic	47% (8)
	3 = multifocal abundant	12% (2)
Regeneration	0 = absent	0% (0)
	1 = focal small	65% (11)
	2 = focal large	24% (4)
	3 = multifocal	12% (2)
Fibrosis	0 = absent	0% (0)
	1 = proliferation of perimysial connective tissue only	0% (0)
	2 = additional mild endomysial fibrosis	41% (7)
	3 = additional moderate endomysial fibrosis	53% (9)
	4 = additional severe endomysial fibrosis	6% (1)

Three domains of pathologic abnormality were chosen for the scoring tool: inflammation, regeneration and fibrosis of 17 patients with LGMD R9 FKRP-related, modified "severity score" from Wedderburn, Varsani, Li, Newton, Amato, Banwell, Bove, Corse, Emslie-Smith, Harding, Hoogendijk, Lundberg, Marie, Minetti, Nennesmo, Rushing, Sewry, Charman, Pilkington, Holton and Group [27], n = number of patients

were CD206$^+$ (Figure 3C) and also MHC class I (Figure 3A) and class II (Figure 3B) as well, and some expressed Siglec-1 (data not shown). Semi-quantitative score demonstrated prevailing CD4 T cells, but more specimens had moderate CD8$^+$ T-cell foci. Macrophages were multifocal and moderately distributed, being also CD206$^+$ (Figure 2D). Cell counts confirmed these findings, showing that macrophages were found with significantly higher numbers than T cells (Figure 2E, Table S1).

To further identify functional profiles of lymphocytes, macrophages, myocytes as well as endothelial and mesenchymal cells, we identified differentially expressed genes by qPCR. In comparison to control muscles that were healthy, we were able to identify significantly elevated levels of gene expression for macrophage markers *CD206* and *CD301* as well as for their respective transcription factors *STAT6* and *STAT3* (Figure 2F). In addition to these, gene expression of Th1 immunity was also investigated. *INOS* as well as *COX2*, *TNFA* and *IL6* were not significantly upregulated (Figure 2G) while *STAT1* reached significance (Figure 2G). *CD4* was also not significantly elevated while *CD8* was elevated in comparison to controls; however, the gene expression for the prototypic Th1, Th2 and Th17 and cytokines such as *IFNG*, *IL12*, *IL13*, *IL21* and *IL17* was only expressed at very low levels in single patients (n = 1–3) and not expressed in NDC patients (data not shown).

We also studied 'anti-inflammatory' *IL10* expression and found elevated levels of this cytokine in LGMD patients in comparison with

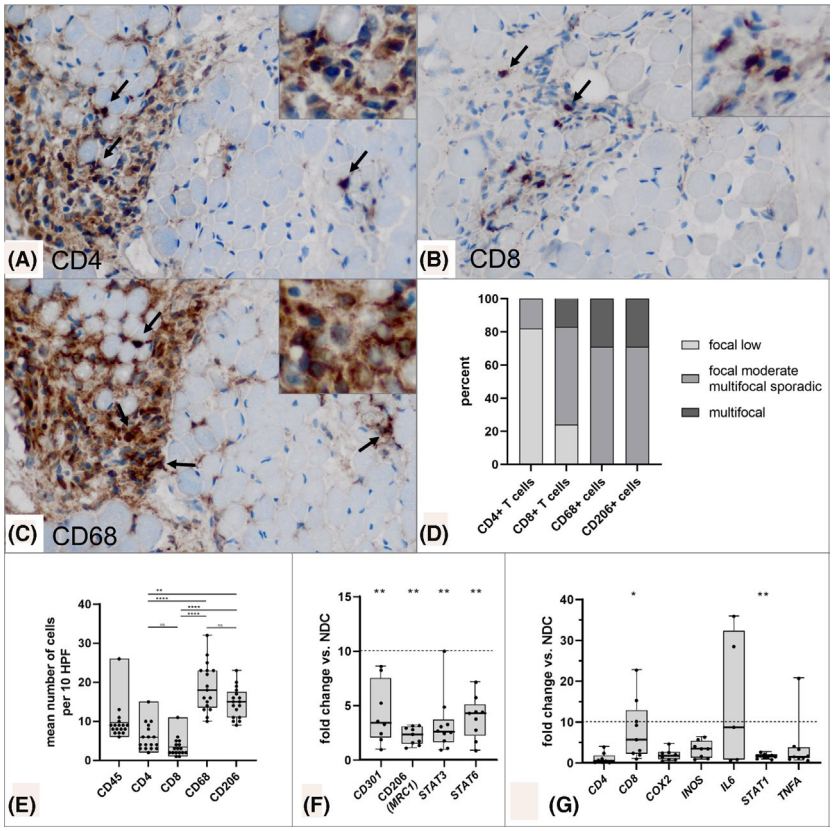

FIGURE 2 Cellular infiltrates mainly consist of T cells and macrophages. Infiltrates consisted of lymphocytes including CD4+ T cells (A), CD8+ T cells (B) and CD68+ macrophages (C). Semi-quantitative scores highlight the distribution from 'diffuse' or 'focal' to 'multifocal' (D). Cell counts further demonstrated that CD68$^+$ macrophages are the predominant cell population (with a mean of approximately 20 cells/HPF, range: 10–32), which were mainly CD206$^+$ (E and S1 table). Gene expression analysis demonstrated elevated mRNA transcript levels for *CD206*, *CD301*, *STAT6* and *STAT3* (F), as well as *STAT1* and *CD8* (G). Other genes were not significantly upregulated (F). Exemplary cells are visualised by black arrows, Original magnification 200x; the significance level was set at $p < 0.05$

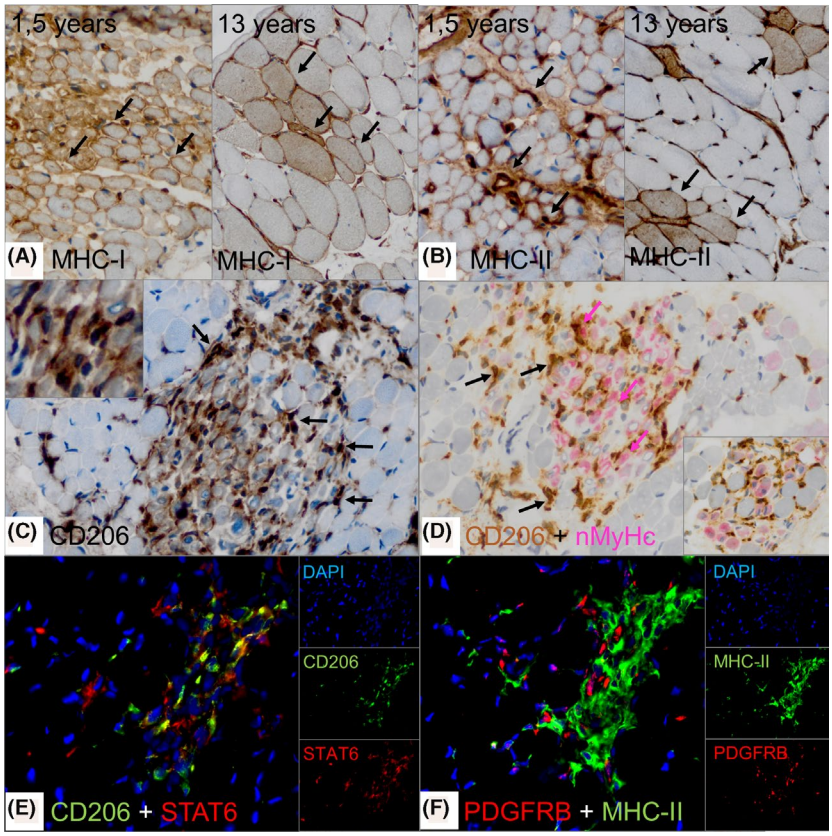

FIGURE 3 Interaction between immune-repressed macrophages regenerating myofibres and vascular structures. MHC class I (A) and class II (B) positive sarcolemmal structures were identified, as were CD206$^+$ macrophages (C, black arrows). Co-staining studies show intimate proximity of CD206$^+$ macrophages (black arrow) with MyHCneo (pink arrow, D). Double labelling of CD206$^+$ macrophages showed expression of STAT6 (E) while PDGFR + pericytes were intermingled with MHC class II + activated macrophages and MHC class II + endothelial cells (F). Original magnification 200×

NDCs. This finding is in line with the assumption that M2-like macrophages as shown here, antagonise M1 polarisation among others by secreting IL-10 (data not shown, because *IL10* was only expressed in single NDCs).

MHC class I and class II positive sarcolemmal structures were also identified with a focal pattern in areas of denser inflammation (Figure 3A,B). CD206$^+$ and Siglec1$^+$ macrophages (Figure 3C), which also expressed MHC class II (data not shown) were lying in close proximity with regenerating neo MHC$^+$ fibres as seen in co-staining studies (Figure 3D). Additionally, CD206$^+$ macrophages expressed STAT6 (Figure 3E) and PDGFRß$^+$ pericytes were located around MHC class II$^+$ activated capillaries residing in close proximity with areas of fibrosis and regenerating fibres (Figure 3F).

Fibrosis is a major feature in LGMDR9

A major issue in LGMDR9 is fibrosis, which may be driven by various factors (discussed below). Expression of VEGF (Figure 4A), for example, was found on many regenerating small myofibres in the respective clusters, and many of these immature neonatal myosin$^+$ fibres co-expressed VEGF (Figure 4B). The above-mentioned macrophages within these regenerating clusters being CD206$^+$ also expressed DAP12, whereas TREM2 expression was upregulated only in some patients, overall indicating a phenotype of immune repression (Figure 4C). In addition to the above-mentioned regenerating myofibres, VEGF also co-labelled many CD206$^+$ macrophages (Figure 4D).

The chemokine CCL18 demonstrating fibrotic activity was intensely stained (Figure 4E). Additionally, gene expression of fibrosis-related markers, which encode key molecules of collagen synthesis such as *IL1B*, *TGFB*, *CCL18*, *P4HA2* (Prolin) and *POSTN* (Periostin), was also (except for IL1B) significantly upregulated in comparison to NDC (Figure 4F).

DISCUSSION

Based on our morphological and gene expression analysis of skeletal muscle biopsies derived from LGMDR9 patients, we identified pathognomonic immune suppressed subpopulations of MHC cl. II$^+$ CD206$^+$ DAP12$^+$ macrophages,[17] and activated MHC cl. II$^+$ and PDGFRβ$^+$ vascular cells admixed with numerous CD4$^+$ T cells within clusters of VEGF$^+$ MHC neonatal$^+$ regenerating myofibres as well as VEGF$^+$CD206$^+$ macrophages. Gene expression studies of skeletal muscle tissue underscored these results by showing significant upregulation of *MRC1*, *CD301* and *STAT6* expression for the specific macrophages, and of *P4HA2*, *POSTN* and *TGFB* expression for fibrosis-related mechanisms. Of note, also gene expression of *STAT1* identifying Th1-mediated immunity and cytotoxic mechanisms was significantly upregulated and highlights the heterogeneity of pathogenic macrophages within the specimen.

We highlighted MHC class I molecules, which are not expressed on the sarcolemma of healthy muscle fibres,[18] with a diffuse sarcolemmal distribution in all LGMDR9-patients' biopsied muscle specimens investigated. We hypothesise that this non-specific but

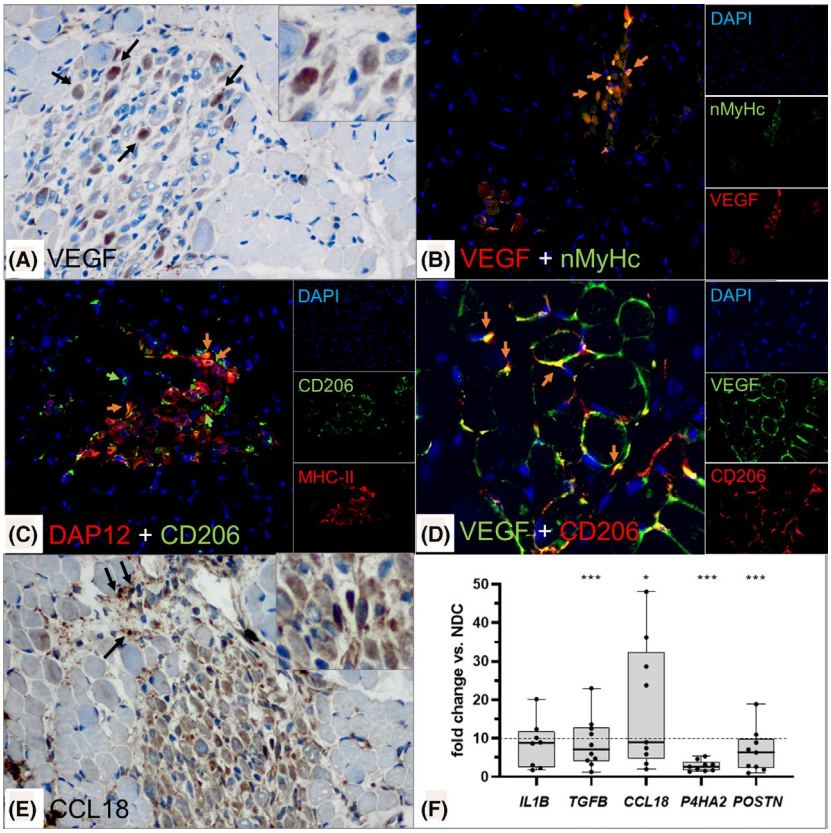

FIGURE 4 Fibrogenesis is enhanced in areas of myogenesis, driven by immune-repressed macrophages in LGMD patients' skeletal muscle biopsies. VEGF is stained in regenerating areas in LGMD patients' biopsies (A) and extensively co-labels with immature MyHCneo + fibres (B, orange arrows = co-labelling). Most CD206$^+$ macrophages co-stained with DAP12$^+$ indicating an immune-repressed phenotype (C, D, green arrow = CD206$^+$ macrophages, orange arrow = co-labelling) while VEGF also co-stains with CD206 macrophages (E, orange arrow = co-labelling). Fibrogenic CCL18 was also intensely stained in regenerating areas of LGMD patients' biopsies (E), and gene expression of many relevant genes, involved in fibrogenesis, was increased (F). Exemplary cells/structures marked by black arrows

highly relevant basic immune activation pattern may be interpreted as a sign of CD8$^+$ T-cell-mediated cytotoxicity in analogy to previous findings with activated (M1) or pro-inflammatory macrophages, arise from exposure to the T-helper (Th)1 cytokines interferon-(IFN) γ and tumour necrosis factor (TNF)-α..[19] Cytotoxic activity was also confirmed by significantly increased *STAT1* expression in the muscle samples. A putative involvement of autoimmune processes was studied by Villalta, Rosenberg and Bluestone for DMD.[20] They discussed an autoimmunological component in DMD pathogenesis, consisting of dystrophin-reactive T cells that are activated by dystrophin from the so-called 'revertant fibres', triggering a specific immune response and involving the above-mentioned molecules.

Interestingly, we also detected MHC class II proteins on the sarcolemma of muscle cells in association with CD4$^+$ T cells, especially in the area of regeneration. The ability of muscle cells for antigen processing and antigen presentation (APC) in combination with MHC class II expression could be shown in inflammatory muscle diseases, and *in vitro* by analysing purified myoblasts stimulated by interferon-gamma.[21] Of note, we expand this knowledge by highlighting the presence of specific immune-repressed CD206$^+$, STAT6$^+$ and DAP12$^+$ macrophages, the expression of MHC class II molecules on muscle fibres, in addition to the significantly increased gene expression of *MRC1*, *CD301*, *STAT6* and *TGFB* ($p < 0.001$) in LGMDR9 patients' muscle tissues specifically. We also highlight that these macrophages cluster among VEGF$^+$ regenerating/immature myofibres, a mechanism which has successfully been studied in mice as well[22,23]: Of note, we also show that a number of those CD206$^+$ macrophages co-express VEGF, which, in turn, links them to an M2-like phenotype involved in fibrogenesis. We also identified a population of activated MHC cl. II$^+$ endothelial cells accompanied by PDGFRβ$^+$ pericytes admixed with those macrophages forming a very focal micromilieu in the regenerating clusters of myofibres. In the lung, the pro-fibrogenic role of PDGFRβ$^+$ pericytes with the 'lung-pericyte-endothelial niche' has also been explored recently.[24]

As we detected specific signs of inflammation, for example (i) inflammatory-regenerative stage with predominance of CD4+/MHC II immune restriction of T cells and (ii) a fibrotic, probably later stage with an additional focal involvement of CD206$^+$ macrophages producing TGFβ) of inflammation, regeneration and fibrosis in all of our patients' biopsied muscle tissues regardless of the age at the time of first manifestation and interval to muscle biopsy, we asked the question if there is any correlation between morphological findings and clinical aspects. However, we did not find any correlation between duration of illness, clinical findings at the time of the biopsy and degree of inflammation, regeneration and fibrosis in the muscle biopsies taken at the age of 4 months–18 years in our cohort.

In the literature, mild inflammatory features consisting of sarcolemmal positivity of MHC class I and small foci of mononuclear cells dominated by CD68$^+$ macrophages, T lymphocytes (t4>t8) and rare eosinophils were described before.[8,25] An in-depth description of the inflammatory response in LGMDR9 patients' muscle tissues was lacking so far.

The specific immune response in LGMDR9 shows similar findings to those obtained in DMD regarding the cellular composition of the inflammatory infiltrates (CD4$^+$ and CD 8$^+$ T cells, macrophages,

expression of MHC class I on muscle cells).[10,26] However, there is a clear difference with respect to the sarcolemmal expression of MHC class II and the specific involvement of the above characterised immune-repressed macrophages involved in regenerative processes in LGMDR9, which has not been described in DMD thus far. However, prominent activation of the complement system on the sarcolemma as described for dysferlinopathies (LGMDR2 dysferlin-related) [27] was not found in LGMDR9 patients' biopsies investigated in this study. Along this line, C5b-9 membrane attack complexes described by Engel and Biesecker[28] in necrotic muscle fibres of DMD patients were neither detected on necrotic fibres nor on the capillaries of our LGMDR9 patients' biopsies studied here. Hence, we conclude that the complement system is not activated in the skeletal muscles of LGMDR9 patients.

In DMD, immune reaction is already activated in preclinical stages.[29-31] The most likely explanation for the successful utilisation of glucocorticoids in DMD is the shift in the macrophage populations from a pro-inflammatory M1 type to an anti-inflammatory M2 phenotype.[26] Of note, in the FKRP, p.P448L mutant mouse model, a regimen of oral prednisolone administration, led to improvement of skeletal muscle damage and enhanced glycosylation of α-DG.[32] Therapeutic assays with corticosteroids showed a positive effect only in single patients, as an individual treatment concept.[25,33] Given that we mainly identified immune-repressed macrophages in all 17 muscle biopsies, this dominance may be a conclusive explanation for the missing effect of glucocorticoids in clinical treatment of LGMDR9 patients.

As immune cells, especially macrophages, are important for tissue homeostasis, especially at borders between the blood stream and organ parenchyma (e.g. CNS),[34] in-depth analysis of the cellular immune responses *in situ*, as an integral part of pathophysiological processes in LGMDR9 is important; last not least when it comes to monitoring pre-clinical and clinical interventional studies such as gene therapy and exon skipping. Identification of specific cellular signatures by cutting edge techniques such as single-cell RNA-sequencing has allowed the identification of highly specific macrophages involved in the 'fibrotic niche' in liver cirrhosis.[17] There is an interesting overlap of cells and molecules involved in fibrosis and immune reactions in their functional analysis and ours, indicating that certain universal activation processes may be relevant in fibrosis and regeneration, such as the TREM2/DAP12 pathway in macrophages (e.g. called $TREM2^{+}CD9^{+}$ 'scar-associated macrophages' in liver fibrosis).

Healthy muscle tissue responds to acute damage with a complex immune response geared towards restitution and evading fibrosis. In a mouse model of acute crush injury, one of the most upregulated genes was *POSTN* (periostin), which suggested that the regeneration process was overwhelmed.[35] Periostin has been recently shown to promote fibroblast migration at the injury site and to favour scar formation. In chronic damage such as muscular dystrophy, the immune response is part of the pathological process with the consequence of fibrotic remodelling and loss of function.[19] The incidence of fibrosis during the course of the disease that we have shown in our LGMDR9 patients had also been described in a previous study.[11] The profibrotic cytokine TGF-β is involved in the regulation of muscle repair via satellite cell activation, controls ECM synthesis, remodelling and degradation, as well as regulation of the immune response intensity.[36] Fibrosis, not only part of the repair process, contributes also to the loss of structure and function of the muscles as an independent pathophysiological factor in mdx-mouse models and DMD patients.[37-39] Symptomatic therapies such as the use of antibodies against connective tissue growth factor (FG-3019), downregulation of TGF-ß by suramin or losartan was under investigation for DMD.[40] Treatment with Postn-nAb is effective for mitigating fibrosis and improving muscle recovery in a mouse model of muscle injury,[41] and could, hence, also be an interesting therapeutic approach in humans with muscular dystrophies like LGMDR9. Persistent fibrosis represents a major obstacle to successful gene- and cell-based therapies for patients with LGMDR9.

Muscle repair is a complex phenomenon needed to recover from damage of any kind, including genetically based membrane dysintegrity. Regeneration and functional restoration of damaged skeletal muscle cells, also called homeostasis, may be crucially regulated by monocytes and local tissue resident macrophages in concert with interacting neighbouring cells such as vascular cells and mesenchymal cells. For the first time, we provide a framework of immune- and regeneration-related processes and cell markers that is fundamental to develop potential targets for therapeutic strategies in patients with LGMDR9—even if they may be supplemental to causative gene restaurative or gene correction attempts.

CONCLUSIONS

Our results underscore the relevance of immune inflammatory features in LGMDR9 and, more specifically, shed light on functional activation or repression of macrophages and their specific role in fibrogenesis and regeneration.

ACKNOWLEDGMENTS

We thank Petra Matylewski for expert technical assistance. Parts of this study (AR and US) were financed in the framework of the NME-GPS project by the European Regional Development Fund (ERDF).

CONFLICT OF INTEREST

All authors report no disclosures.

AUTHORS' CONTRIBUTIONS

HK: study design, patient acquisition and writing of manuscript; CP: generation of data and writing of manuscript; LB: generation of data and patient acquisition; AvM: manuscript revision; MS: patient acquisition, analysis of genetic data and manuscript revision; ADM: patient acquisition and manuscript revision; AR: manuscript

revision; HHG: manuscript revision; US: patient acquisition and manuscript revision; WS: study design, data acquisition and writing of the manuscript.

ETHICAL APPROVAL

Written informed consent was obtained from the participants (or rather their legal guardians) for the participation to subsequent research as well as for publication of the findings (including any potentially identifying information). Ethical approval for this retroactive study was obtained from both Universities (Essen/Berlin) AZ 14–6175-BO and EA1/204/11 and EA1/170/11.

PEER REVIEW

The peer review history for this article is available at https://publons.com/publon/10.1111/nan.12730.

DATA AVAILABILITY STATEMENT

The data that support the findings of this study are available from the corresponding author upon reasonable request.

ORCID

Heike Kölbel https://orcid.org/0000-0001-9629-7053
Markus Schuelke https://orcid.org/0000-0003-2824-3891
Andreas Roos https://orcid.org/0000-0003-2833-0928
Werner Stenzel https://orcid.org/0000-0002-1143-2103

REFERENCES

1. Norwood FL, Harling C, Chinnery PF, Eagle M, Bushby K, Straub V. Prevalence of genetic muscle disease in Northern England: in-depth analysis of a muscle clinic population. *Brain*. 2009;132(Pt 11):3175-3186.
2. Stensland E, Lindal S, Jonsrud C, et al. Prevalence, mutation spectrum and phenotypic variability in Norwegian patients with Limb Girdle Muscular Dystrophy 2I. *Neuromuscul Disord*. 2011;21(1):41-46.
3. Richard I, Laurent J-P, Cirak S, Vissing J, Group EFS. 216th ENMC international workshop: clinical readiness in FKRP related myopathies January 15–17, 2016 Naarden, The Netherlands. *Neuromuscul Disord*. 2016;26(10):717-724.
4. Brockington M, Yuva Y, Prandini P, et al. Mutations in the fukutin-related protein gene (FKRP) identify limb girdle muscular dystrophy 2I as a milder allelic variant of congenital muscular dystrophy MDC1C. *Hum Mol Genet*. 2001;10(25):2851-2859.
5. Kanagawa M, Toda T. Muscular dystrophy with ribitol-phosphate deficiency: a novel post-translational mechanism in dystroglycanopathy. *J Neuromuscular Dis*. 2017;4(4):259-267.
6. Ervasti JM, Campbell KP. A role for the dystrophin-glycoprotein complex as a transmembrane linker between laminin and actin. *J Cell Biol*. 1993;122(4):809-823.
7. Esapa CT, Benson MA, Schroder JE, et al. Functional requirements for fukutin-related protein in the Golgi apparatus. *Hum Mol Genet*. 2002;11(26):3319-3331.
8. Boito CA, Fanin M, Gavassini BF, Cenacchi G, Angelini C, Pegoraro E. Biochemical and ultrastructural evidence of endoplasmic reticulum stress in LGMD2I. *Virchows Arch*. 2007;451(6):1047-1055.
9. Tidball JG, Villalta SA. Regulatory interactions between muscle and the immune system during muscle regeneration. *Am J Physiol Regul Integr Comp Physiol*. 2010;298(5):R1173-R1187.
10. Tidball JG, Welc SS, Wehling-Henricks M. Immunobiology of inherited muscular dystrophies. *Comprehensive Physiol*. 2018;8(4):1313-1356.
11. Alhamidi M, Brox V, Stensland E, Liset M, Lindal S, Nilssen Ø. Limb girdle muscular dystrophy type 2I: no correlation between clinical severity, histopathology and glycosylated α-dystroglycan levels in patients homozygous for common FKRP mutation. *Neuromuscul Disord*. 2017;27(7):619-626.
12. Vannoy CH, Xiao W, Lu P, Xiao X, Lu QL. Efficacy of gene therapy is dependent on disease progression in dystrophic mice with mutations in the FKRP gene. *Molecular Therap Methods Clin Develop*. 2017;5:31-42.
13. Cataldi MP, Lu P, Blaeser A, Lu QL. Ribitol restores functionally glycosylated α-dystroglycan and improves muscle function in dystrophic FKRP-mutant mice. *Nat Commun*. 2018;9(1):3448.
14. Brockington M, Blake DJ, Prandini P, et al. Mutations in the fukutin-related protein gene (FKRP) cause a form of congenital muscular dystrophy with secondary laminin alpha2 deficiency and abnormal glycosylation of alpha-dystroglycan. *Am J Hum Genet*. 2001;69(6):1198-1209.
15. Wedderburn LR, Varsani H, Li CKC, et al. International consensus on a proposed score system for muscle biopsy evaluation in patients with juvenile dermatomyositis: a tool for potential use in clinical trials. *Arthritis Rheum*. 2007;57(7):1192-1201.
16. Preuße C, von Moers A, Kölbel H, et al. Inflammation-induced fibrosis in skeletal muscle of female carriers of Duchenne muscular dystrophy. *Neuromuscul Disord*. 2019;29(7):487-496.
17. Ramachandran P, Dobie R, Wilson-Kanamori JR, et al. Resolving the fibrotic niche of human liver cirrhosis at single-cell level. *Nature*. 2019;575(7783):512-518.
18. Evans NP, Misyak SA, Robertson JL, Bassaganya-Riera J, Grange RW. Immune-mediated mechanisms potentially regulate the disease time-course of duchenne muscular dystrophy and provide targets for therapeutic intervention. *J Injury, Func, Rehab*. 2009;1(8):755-768.
19. Mann CJ, Perdiguero E, Kharraz Y, et al. Aberrant repair and fibrosis development in skeletal muscle. *Skelet Muscle*. 2011;1(1):21.
20. Villalta SA, Rosenberg AS, Bluestone JA. The immune system in Duchenne muscular dystrophy: friend or foe. *Rare Diseases (Austin, Tex)*. 2015;3(1):e1010966.
21. Wiendl H, Lautwein A, Mitsdörffer M, et al. Antigen processing and presentation in human muscle: cathepsin S is critical for MHC class II expression and upregulated in inflammatory myopathies. *J Neuroimmunol*. 2003;138(1–2):132-143.
22. Arnold L, Henry A, Poron F, et al. Inflammatory monocytes recruited after skeletal muscle injury switch into antiinflammatory macrophages to support myogenesis. *J Exp Med*. 2007;204(5):1057-1069.
23. Saclier M, Yacoub-Youssef H, Mackey AL, et al. Differentially activated macrophages orchestrate myogenic precursor cell fate during human skeletal muscle regeneration. *Stem cells (Dayton, Ohio)*. 2013;31(2):384-396.
24. Wilson CL, Stephenson SE, Higuero JP, Feghali-Bostwick C, Hung CF, Schnapp LM. Characterization of human PDGFR-β-positive pericytes from IPF and non-IPF lungs. *Am J Physiol Lung Cell Mol Physiol*. 2018;315(6):L991-l1002.
25. Darin N, Kroksmark AK, Ahlander AC, Moslemi AR, Oldfors A, Tulinius M. Inflammation and response to steroid treatment in limb-girdle muscular dystrophy 2I. *Eur J Paediatric Neurol*. 2007;11(6):353-357.
26. De Paepe B, Creus KK, Martin JJ, De Bleecker JL. Upregulation of chemokines and their receptors in Duchenne muscular dystrophy: potential for attenuation of myofiber necrosis. *Muscle Nerve*. 2012;46(6):917-925.
27. Brunn A, Schröder R, Deckert M. The inflammatory reaction pattern distinguishes primary dysferlinopathies from idiopathic

inflammatory myopathies: an important role for the membrane attack complex. *Acta Neuropathol*. 2006;112(3):325-332.
28. Engel AG, Biesecker G. Complement activation in muscle fiber necrosis: demonstration of the membrane attack complex of complement in necrotic fibers. *Ann Neurol*. 1982;12(3):289-296.
29. Chen YW, Nagaraju K, Bakay M, et al. Early onset of inflammation and later involvement of TGFbeta in Duchenne muscular dystrophy. *Neurology*. 2005;65(6):826-834.
30. Spencer MJ, Montecino-Rodriguez E, Dorshkind K, Tidball JG. Helper (CD4(+)) and cytotoxic (CD8(+)) T cells promote the pathology of dystrophin-deficient muscle. *Clin Immunol*. 2001;98(2):235-243.
31. Mendell JR, Campbell K, Rodino-Klapac L, et al. Dystrophin immunity in Duchenne's muscular dystrophy. *N Engl J Med*. 2010;363(15):1429-1437.
32. Wu BO, Shah SN, Lu P, et al. Glucocorticoid steroid and alendronate treatment alleviates dystrophic phenotype with enhanced functional glycosylation of α-dystroglycan in mouse model of limb-girdle muscular dystrophy with FKRPP448L mutation. *Am J Pathol*. 2016;186(6):1635-1648.
33. Lin Y-C, Murakami T, Hayashi YK, et al. A novel FKRP gene mutation in a Taiwanese patient with limb-girdle muscular dystrophy 2I. *Brain Develop*. 2007;29(4):234-238.
34. Utz SG, See P, Mildenberger W, et al. Early fate defines microglia and non-parenchymal brain macrophage development. *Cell*. 2020;181(3):557-73.e18.
35. Ceafalan LC, Dobre M, Milanesi E, et al. Gene expression profile of adhesion and extracellular matrix molecules during early stages of skeletal muscle regeneration. *J Cell Mol Med*. 2020;24(17):10140-10150.
36. Delaney K, Kasprzycka P, Ciemerych MA, Zimowska M. The role of TGF-β1 during skeletal muscle regeneration. *Cell Biol Int*. 2017;41(7):706-715.
37. Zhou L, Porter JD, Cheng G, et al. Temporal and spatial mRNA expression patterns of TGF-beta1, 2, 3 and TbetaRI, II, III in skeletal muscles of mdx mice. *Neuromuscul Disord*. 2006;16(1):32-38.
38. Zanotti S, Gibertini S, Di Blasi C, et al. Osteopontin is highly expressed in severely dystrophic muscle and seems to play a role in muscle regeneration and fibrosis. *Histopathology*. 2011;59(6):1215-1228.
39. Song Y, Yao S, Liu Y, et al. Expression levels of TGF-β1 and CTGF are associated with the severity of Duchenne muscular dystrophy. *Exp Therap Med*. 2017;13(4):1209-1214.
40. Crone M, Mah JK. Current and emerging therapies for duchenne muscular dystrophy. *Curr Treat Options Neurol*. 2018;20(8):31.
41. Hara M, Yokota K, Saito T, et al. Periostin promotes fibroblast migration and inhibits muscle repair after skeletal muscle injury. *J Bone Joint Surg*. 2018;100(16):e108.

SUPPORTING INFORMATION

Additional supporting information may be found online in the Supporting Information section.

Table S1

How to cite this article: Kölbel H, Preuße C, Brand L, et al. Inflammation, fibrosis and skeletal muscle regeneration in LGMDR9 are orchestrated by macrophages. *Neuropathol Appl Neurobiol*. 2021;47:856–866. https://doi.org/10.1111/nan.12730